

# A Comprehensive Model for Stiffness Coefficients in V-Shaped Cantilevers

A. H. Korayem<sup>\*1</sup>, A. K. Hoshiar<sup>2</sup>, S. Badrlou<sup>1</sup>, and M. H. Korayem<sup>1</sup>

1. Robotic Research Laboratory, Center of Excellence in Experimental Solid Mechanics and Dynamics, School of Mechanical Engineering, Iran University of Science and Technology, Narmak, Tehran, I. R. Iran
2. Faculty of Industrial and Mechanical Engineering, Islamic Azad University, Qazvin Branch, Qazvin, I. R. Iran

(\*) Corresponding author: hkorayem@iust.ac.ir  
(Received: 01 Nov 2014 and Accepted: 10 Jan. 2016)

## Abstract

During past decade the AFM based nanomanipulation has been focus of attention as the promising nano fabrication approach. The main challenge in this process is the real-time monitoring. Consequently, the dynamic models have been proposed as a solution to the existing challenge. In the modeling approach the magnitudes of the forces are proportional to the stiffness coefficients of cantilevers. The precise calculation of these coefficients has been introduced in numerous works. The proposed stiffness coefficients for the V-shaped cantilevers fail to present in all commercial cantilever geometry. The geometrical deviation has a considerable impact on the magnitude of stiffness coefficients. Therefore, in this paper the existing model has been modified to include the commercial cantilever and take into account the effect of geometry variation. FEM simulation has been used to investigate the effect of geometry change and the results of these simulations have been exerted to the model which resulted in proposed comprehensive model. The proposed new stiffness model covers a wide range of commercial V-shape cantilevers and makes the process more practical.

**Keywords:** Atomic force microscope; V-shaped cantilever; stiffness coefficients.

## 1. INTRODUCTION

Atomic Force Microscope (AFM) is one of the primary instruments for investigation of surface topographies; however, it can also act as a nanomanipulator to push nano particles and manufacture nano structure; thus, it is very important to know the dynamics of the AFM in order to achieve a reliable and efficient manipulation process [1]. In the controlled manipulation of nanoparticles, tip of cantilever pushes the particle till it reaches the desired location. Throughout the process of manipulation by the AFM, the manipulation forces are measured based on the deformation of the cantilever. Therefore, to have a successful process, it is vital to measure spring constants precisely.

One of the parameters involved in the accuracy and precision of nanoparticles displacement operations is the stiffness coefficient of cantilevers. The modeling of

stiffness coefficient for rectangular, V-shaped and dagger-shaped cantilevers, has been studied by innumerable researches. Experimental, numerical and theoretical techniques have been applied to formulate the stiffness models. In this paper, a comprehensive stiffness model for practical V-shaped cantilevers has been introduced.

The computation of static deformations of cantilever plates is a fundamental principle in the use of atomic force microscope (AFM). Static test methods have already been considered for obtaining a cantilever's stiffness coefficient. In one method, a mass is hung from the free end of the cantilever and the static displacement is measured. Then by using the force-displacement relationship, the normal stiffness coefficient of every cantilever with arbitrary shape is

determined [2]. Also, the displacement of the cantilever tip is determined comparing with a reference cantilever, and the normal stiffness coefficient of the considered cantilever is obtained [3-6]. By using the plate deformation theory, Sader and White presented approximate formulas for the static displacement of cantilevers and they evaluated the obtained results by the theoretical solution through the finite element method [7]. Using the dynamics of added mass to cantilever and the resonant frequency and analysis of thermal noise in a body are the dynamic and non-destructive testing methods that are used for finding the normal stiffness of cantilevers with arbitrary geometries [8-11].

In another technique, the theory of parallel beam approximation (PBA) has been used. Despite its limitations, because of its simplicity of analytical computations, this method is commonly used in finding the spring constant of the V-shaped cantilever in the atomic force microscope [12]. Different methods of calibration of AFM cantilevers with respect to accuracy and precision have been compared [13, 14]. Neumeister offered an analytical model for determining the longitudinal, lateral and normal stiffness coefficients of a V-shaped cantilever and compared the results with the values obtained from the finite element method and showed that the presented equations are very accurate for determining the stiffness coefficients for the cantilever of specific geometry [15]. Green and Sader have attempted to improve the accuracy of the V-shaped cantilever's stiffness coefficients [16]. Regarding the stiffness coefficients of the V-shaped cantilever, Clifford and Seah have concentrated more on the cantilever's triangular section [17].

Sader et al. employed the hydrodynamic functions in experiments to calculate the stiffness values of nonrectangular and irregular cantilevers which are actually used in practice [18]. In recent research works, Korayem and Daeinabi investigated

the V-shaped, rectangular and dagger-shaped cantilevers and explored the effects of all the influential factors such as thickness, width, length and tip-to-free end distance of the ideal cantilevers on the stiffness coefficients in the main directions [19, 20]. The stiffness of V-shape cantilever has been studied using an experimental setup by Rui et.al [21]. The modeling of V-shape cantilever and its effect on critical forces on manipulation of biological particles has been studied by Daeinabi et.al [22]. The effect of piezo layers on stiffness and dynamic has been investigated by Koreyem and Ghaderi [23]. The stiffness coefficients model of V-shaped cantilevers is limited to the ideal form so in this paper the exciting model has been improved to present the model for different from of V-shaped cantilevers. Due to the analytical model restrictions, FEM simulations have been used to develop the new model.

In this paper, a general comprehensive model for stiffness coefficients has been developed. The stiffness coefficients of V-shaped cantilevers in different geometries are obtained using the FEM method. These coefficients are then compared with the values obtained in analytical reports and finally by using the correction coefficients, the modeling of stiffness coefficients is improved.

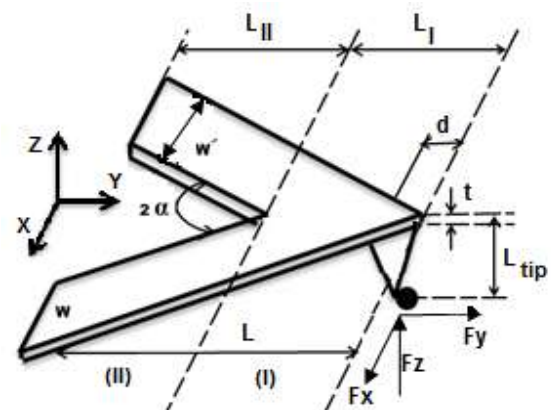


**Figure.1.** The V-shaped cantilever used in the AFM consists of the triangular section (I) and two oblique rectangular beams (II) [15].

## 2. MODELLING THE FORCES APPLIED ON THE V-SHAPED CANTILEVER

In this section, by using the model of a V-shaped cantilever, the deformations of the cantilever under the effect of force is investigated and a 3D model is presented. In this analysis, three forces are applied to the probe tip along the three X, Y and Z directions (Figure.1) [15, 19].

### 2.1. Modeling of the normal stiffness coefficient ( $K_z$ )

Considering the method conducted by Neumeister, the normal stiffness coefficient of the cantilever (in Z direction) will be as follows [15,19]:

$$K_Z = F_z [Z_I + Z_{II} + \theta_{II} (\frac{w'}{\sin \alpha} - d)]^{-1} \quad (1)$$

$$Z_I = (\frac{6F_Z L_I}{Ew't^3}) [\frac{(L_I - d)^2}{2} + d(L_I - d)(\ln(\frac{d}{L_I}) - 1) + L_I d \ln(\frac{L_I}{d})] \quad (2)$$

$$Z_{II} = (\frac{F_Z L_{II}^2}{Ew't^3 \cos^2 \alpha}) [\frac{2L_{II}}{\cos \alpha} + 3(w' \cot \alpha - d \cos \alpha - r \sin \alpha)] \quad (3)$$

$$\theta_{II} = (\frac{3F_Z L_{II}(1+\nu)}{Ew't^3 \cos \alpha}) (\frac{w'}{\sin \alpha} - d + r \cot \alpha) \quad (4)$$

$$r = \frac{(L_{II} \tan \alpha + (w' - d \sin \alpha)(1 - \nu) \cos \alpha)}{(2 - (1 - \nu) \cos^2 \alpha)} \quad (5)$$

Where  $\alpha$ ,  $w'$  and  $d$  respectively are the half of the angle of tip, the width of the two bases and distance from end of the cantilever,  $L_I$  is the length of the cantilever's triangular plate,  $\nu$  is *Poisson's ratio*,  $Z_I$  is the deformation of the triangular plate (I),  $Z_{II}, \theta_{II}$  are the

deformation and the bending angle in the junction of the two parts (II&I), respectively and  $b = 2[L \times \tan(\alpha) - w]$ ,

$$L_{II} = L(1 - 2\frac{w}{b}), \quad L_I = \frac{w}{\tan \alpha} \quad \text{and} \\ L = L_I + L_{II}.$$

### 2.2. Modeling of the cantilever's lateral stiffness coefficient ( $K_x$ )

The spring constant of the V-shaped cantilever in the X direction is calculated from the bending and twisting caused by force  $F_x$  and the bending stiffness resulting from this force is obtained as follows [15,19]:

$$K_x^{bend} = Et(\alpha - \sin \alpha \cos \alpha) (\ln(\frac{L}{d}))^{-1} \quad (6)$$

The rotation of the triangular plate around the X axis which is produced by moment  $T$  ( $T = F_x \times L_{tip}$ ) is as follows:

$$\phi_I = (\frac{3T(1+\nu)}{Et^3 \tan \alpha}) \log(\frac{w'}{d \sin \alpha}) \quad (7)$$

$$\phi_{II} = (\frac{3TL_{II}(1+\nu) \cos \alpha}{Ew't^3}) [1 - (6L_{II}w' \sin \alpha + \frac{3w'^2(1+\nu) \cos^2 \alpha}{8L_{II}^2} + 3w'^2(1+\nu) \cos^2 \alpha)] \quad (8)$$

$$K_x^{tors} = \frac{K_\phi}{L_{tip}^2} = (\frac{Et^3}{3(1+\nu)L_{tip}^2}) (\frac{\log(\frac{w'}{d \sin \alpha})}{\tan \alpha} + \frac{L_{II} \cos \alpha}{w'} - \frac{3 \sin 2\alpha}{8})^{-1} \quad (9)$$

$$K_x = \frac{K_x^{bend} \times K_x^{tors}}{K_x^{bend} + K_x^{tors}} \quad (10)$$

$\phi_I$  and  $\phi_{II}$  indicates the rotation of the triangular plate (I) and oblique beams (II). The twisting stiffness becomes:

$$K_\phi = \frac{T}{(\phi_I + \phi_{II})}; \text{ and total lateral stiffness}$$

will be as follows:

### 2.3. Modeling of the cantilever's longitudinal stiffness coefficient ( $K_y$ )

Finally, the effect of the force in the Y direction ( $F_y$ ) is presented. The longitudinal deformation of the cantilever has been disregarded, because it is very small displacement; so only the coefficient of stiffness resulting from net moment  $M = F_y \times L_{tip}$  due to force  $F_y$  along the Y axis is considered [15, 19]:

$$\theta_I = \left( \frac{6M}{Et^3 \tan \alpha} \right) \log \left( \frac{w'}{d \sin \alpha} \right) \quad (11)$$

$$\theta_{II} = \frac{6ML_{II}(1+\nu)}{Et^3 w' (2 - (1-\nu) \cos^2 \alpha)} \quad (12)$$

In the above relation  $\theta_I$  and  $\theta_{II}$  are the rotations of the triangular plate and the two oblique beams, respectively.

$$K_Y = \left\{ \left[ \frac{6}{Et^3 \tan \alpha} \log \left( \frac{w'}{d \sin \alpha} \right) + \frac{6L2(1+\nu)}{Ew't^3 (2 - (1-\nu) \cos^2 \alpha)} \right] L_{tip}^2 \right\}^{-1} \quad (13)$$

## 3. INVESTIGATING THE NEW GEOMETRICAL MODELS

In this paper, the finite element simulation has been employed to obtain the static displacements. As it is demonstrated in Figure 2 the X parameter varies between 0 to 50  $\mu m$ . Then, the force applied on the tip of the cantilever and the constraints applied to the other end. Using the deformation results and applied forces, the stiffness coefficients ( $K_x$ ,  $K_y$  and  $K_z$ )

have been obtained (3D, 20 node structural element has been used for FEM simulation). To calculate the cantilever stiffness coefficients in the three directions of X, Y and Z, the forces of  $F_x$ ,  $F_y$  and  $F_z$  are respectively applied on the tip of the V-shaped cantilever and the static displacements in these three directions are obtained using FEM method. Now, since the displacement is equal to  $\left( \frac{F}{K} \right)$ , by

having the values of the force and the displacement, the stiffness coefficients of  $K_x$ ,  $K_y$  and  $K_z$  are determined. Considering the geometrical variations in the cantilever according to Fig. 2, the changes of stiffness coefficients  $K_x$ ,  $K_y$  and  $K_z$  have been presented (Fig. 2) relative to the other stiffness coefficients, the lateral stiffness coefficient  $K_x$  is highly sensitive to the changes of the geometrical variations. Also, as it has been pointed out, stiffness coefficient  $K_z$  has a lower sensitivity to the geometrical changes of the V-shaped cantilever [7]. The effects of variation in thickness, length and width have also been investigated using FEM method. For the ideal cantilever ( $X=0$ ) the result of FEM simulation in X, Y and Z directions are in harmony with Neumeister model. However, the model failed to estimate the accurate stiffness coefficient with the change in cantilever geometry (parameter X) but as it is demonstrated in Figs. 3 and 4 the rate of change in stiffness coefficient for both FEM method and the modeling, are similar [15]

## 4- VALIDATING THE MODELING OF FORCES APPLIED ON THE CANTILEVER

In order to validate the presented simulation, a finite element model of the V-shaped cantilever with the dimensions shown in Table 1 has been used. For validation purposes, the results obtained from this simulation are compared with those of the Neumeister and Ducker's model.

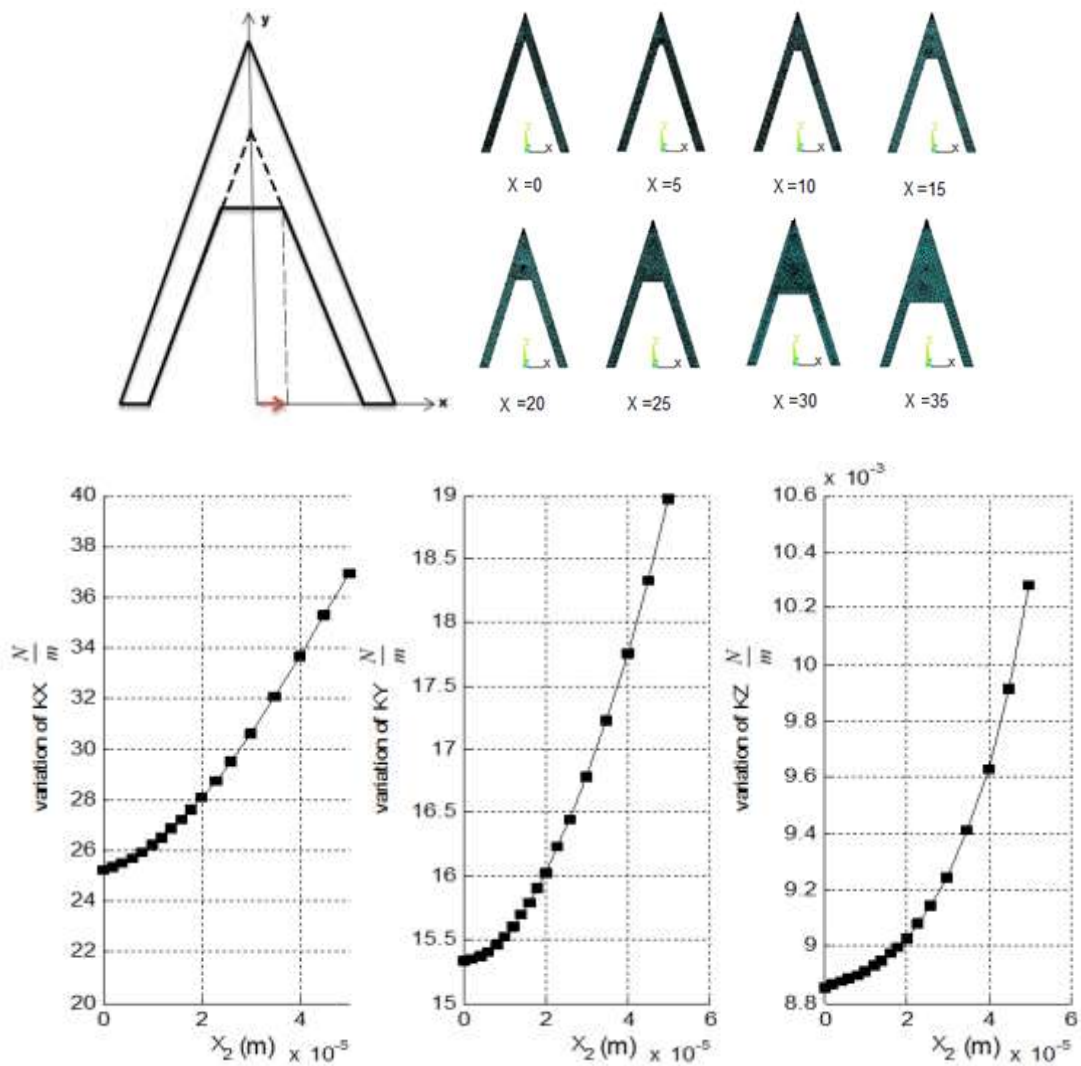


**Figure2.** The presented model, Geometrical changes of the finite element modeling and changes of K<sub>x</sub>, K<sub>y</sub> and K<sub>z</sub> versus X

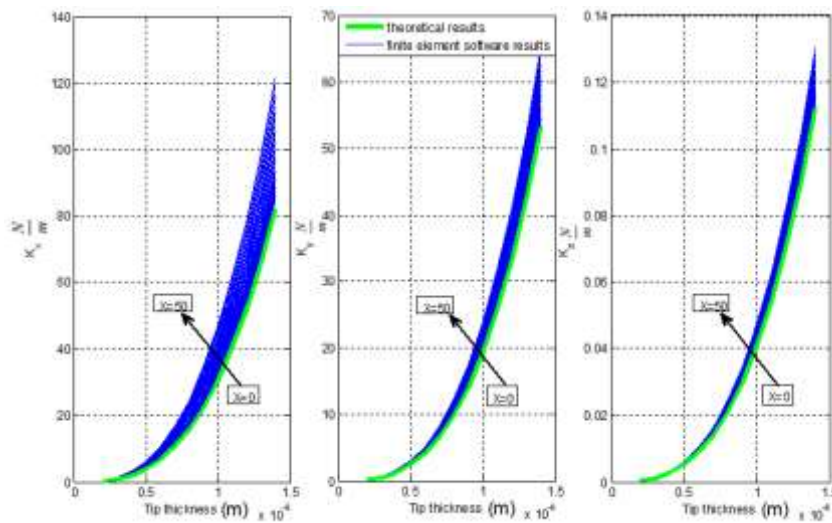


**Figure3.** Stiffness coefficients of variation for the cantilever thickness (X is in terms of micrometer)

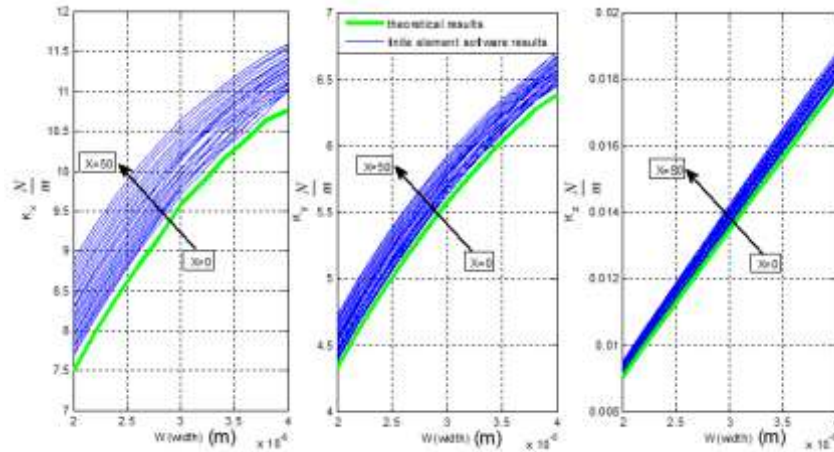


**Figure4.** Stiffness coefficients of variation for the cantilever width ( $X$  is in terms of micrometer)

**Table1.** Geometrical values and mechanical properties of the V-shaped cantilever

Geometric features						Physical features		
	L	W	t	d	$\alpha$	E	N	
	4.2( $\mu\text{m}$ )	323( $\mu\text{m}$ )	20( $\mu\text{m}$ )	0.6( $\mu\text{m}$ )	12( $\mu\text{m}$ )	28(Deg.)	143(G.Pa)	0.33

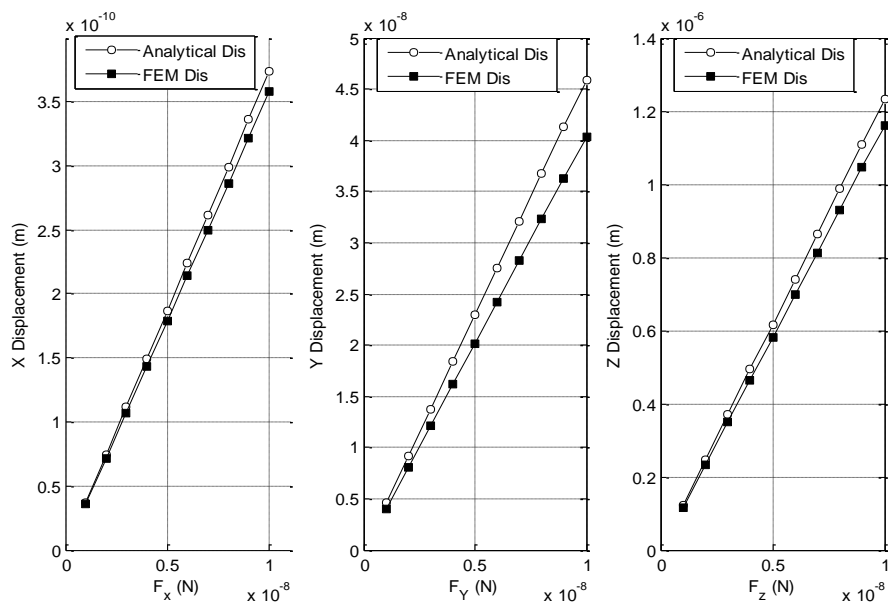


**Figure5.** Comparison between force-displacement diagrams along the  $X$ ,  $Y$  and  $Z$  direction obtained by the analytical and finite element methods

Considering the force-displacement diagrams for the ideal V-shaped cantilever in Fig. 5, it is observed that the  $X$ -direction displacements obtained by the analytical and finite element methods are identical. Regarding the force-displacement diagram

along the  $Y$  direction, the two diagrams have a slight difference, which could be due to not considering the cantilever's longitudinal deformation in the  $Y$  direction. It is also observed that the two diagrams in the  $Z$  direction are in harmony.

## 5. CORRECTION FACTORS DETERMINATION

Dividing the stiffness coefficient resulted from FEM simulation and ideal stiffness coefficient, the correction factors for the cantilever in three directions are depicted in Figure. 6. These correction factors are dimensionless ( $X$  is the geometry parameter presented in Figure. 1).

$$\begin{aligned}
 Kx_{NEW} &= [1 + 1.5(\frac{x}{b})]Kx = [1 + 1.5(\frac{x}{b})] \\
 &[[Kx^{bend}]^{-1} + [Kx^{tors}]^{-1}]^{-1} = [1 + 1.5(\frac{x}{b}) \\
 &[[Et(\alpha - \sin \alpha \cos \alpha)(\ln(\frac{L}{d}))^{-1}]^{-1} + \\
 &[(\frac{Et^3}{3(1+\nu)L^2_{tip}})(\frac{\log(\frac{w'}{d \sin \alpha}}{\tan \alpha}) \\
 &+ \frac{L_{II} \cos \alpha}{w'} - \frac{3 \sin 2\alpha}{8})^{-1}]^{-1}]^{-1} \quad (14)
 \end{aligned}$$

To make the proposed dimensionless correction factor, ( $X/b$ ) has been used as the variable, and a first, second and third order polynomials have been proposed to approximate the result in Figure. 6. These correction factors are used as multiplier terms to the stiffness values obtained by Neumeister and Ducker for ideal cantilevers and yield a new comprehensive model, which is feasible for practical V-shaped cantilevers. The new comprehensive model for practical V-shaped cantilevers, with respect to geometrical changes (equivalent to the changes in the value of  $X$ ), are as follows ( $b$  is cantilever width and  $X$  is the changing geometrical parameters (shown in Figures 1 and 2, respectively)). Similarly, the corrected factors are multiplied by the longitudinal stiffness coefficient ( $Ky$ ) and normal stiffness coefficient ( $Kz$ ), respectively, and yield geometry-dependent stiffness coefficients model.

$$\begin{aligned}
 Ky_{NEW} &= [1 + 2(\frac{x}{b})^2]Ky = \\
 &[1 + 2(\frac{x}{b})^2] \{ [\frac{6}{Et^3 \tan \alpha} * \log(\frac{w'}{d \sin \alpha}) + \\
 &\frac{6L2(1+\nu)}{EWt^3(2-(1-\nu)*\cos^2 \alpha)}] * L^2_{tip} \}^{-1} \quad (15)
 \end{aligned}$$

$$\begin{aligned}
 Kz_{NEW} &= [1 + (\frac{2x}{b})^3] \times Kz = [1 + (\frac{2x}{b})^3]: \\
 &F_z[Z_I + Z_{II} + \theta_{II}(\frac{w'}{\sin \alpha} - d)]^{-1} = \\
 &[1 + (\frac{2x}{b})^3] \times \{ (\frac{6L_I}{Ewt^3})[\frac{(L_I - d)^2}{2} + \\
 &d(L_I - d)(\ln(\frac{d}{L_I}) - 1) + L_I d \ln(\frac{L_I}{d})] + \\
 &(\frac{L^2_{II}}{Ew't^3 \cos^2 \alpha})[\frac{2L_{II}}{\cos \alpha} + 3(w' \cot \alpha - \\
 &d \cos \alpha - r \sin \alpha)] + (\frac{3L_{II}(1+\nu)}{Ew't^3 \cos \alpha}) \\
 &(\frac{w'}{\sin \alpha} - d + r \cot \alpha)(\frac{w'}{\sin \alpha} - d) \}^{-1} \quad (16)
 \end{aligned}$$

Finally, according to Figure. 7, the new stiffness coefficients in three main coordinate directions have been presented with respect to geometrical changes and compared with the results obtained from the FEM simulation. For stiffness coefficient  $Kx$ , the value obtained in the ideal case ( $X = 0$ ), the data obtained by the finite element method and by equation (14) are almost identical. As is observed in Figure. 7, the values of  $Kx$  are higher relative to the other two stiffness values. For the new  $Ky$ , at  $X < 25 \mu m$ , the changes occur with a mild slope, and for a larger geometrical change, we will witness a high sensitivity to this geometrical parameter. In the proposed  $Kz$  a minor change in stiffness has been observed.

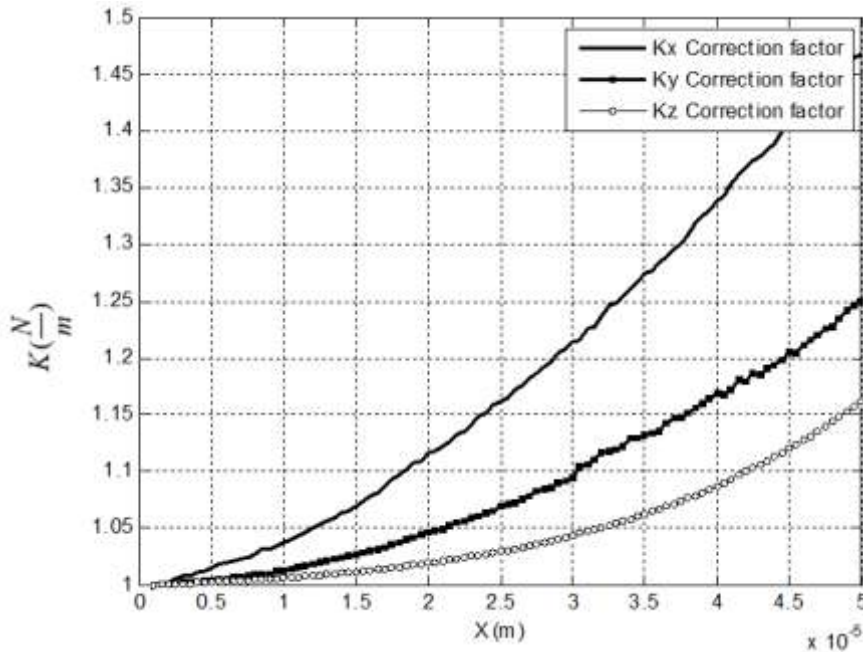


**Figure6.** Correction factor for stiffness coefficient  $K_x$ ,  $K_y$  and  $K_z$

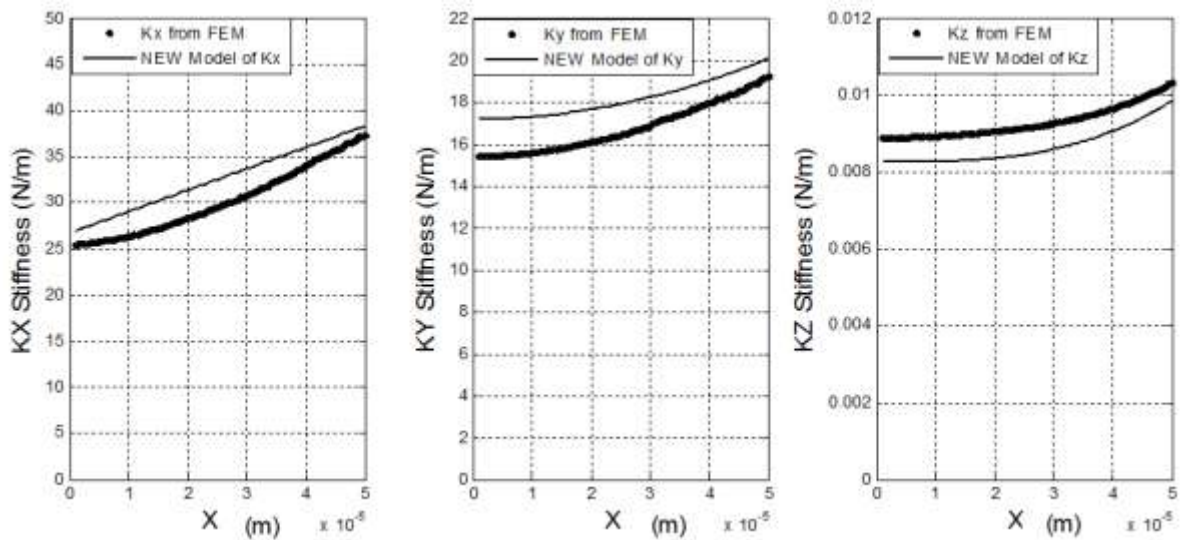


**Figure7.** Comparison between the modified stiffness coefficient of  $K_x$ ,  $K_y$ ,  $K_z$  and the result obtained from the finite element analysis

As is observed, the stiffness values obtained from the new theory correlate very closely with the data obtained from the finite element approach (there is a minor deviation which is in acceptable limits); consequently, both results are in harmony. The gaps formed in the diagrams are due to FEM simulation errors and also the assumptions in the theoretical formulas which can be neglected.

## 6. CONCLUSION

The real-time monitoring limitation is the most important barrier in AFM based nano manipulation. Consequently, to develop a practical manipulation strategy, modeling and simulation of the process have been heavily investigated in numerous researches. For a successful manipulation by the means of AFM nano robot, it is of great importance to have an accurate dynamic model and to have precise

dynamic model, stiffness coefficient should be determined accurately.

The cantilever geometry varies as a result of existing manufacturing errors in commercial cantilevers which have a huge impact on cantilever stiffness. Based on the simulations 44%, 23% and 31% change of  $K_x$ ,  $K_y$  and  $K_z$  is obtained, respectively. Therefore, in this paper the exciting stiffness model with the use of FEM simulation has been further improved to include effect of cantilever geometry.

With the use of presented model, it is possible to predict the stiffness coefficients ( $K_x$ ,  $K_y$  and  $K_z$ ) for a deviation of  $X$  between 0 to 50  $\mu m$ . The developed model enables us to predict stiffness coefficients for a wide range of commercial cantilevers. The developed model shows acceptable consistency (less than 1.5 % deviation) and enables us to model stiffness coefficient precisely.

## REFERENCES

1. Binnig, G., Quate, C.F., Gerber, C. (1986). "Atomic force microscope" *Phys. Rev. Lett.*, 56: 930-933.
2. Senden, T., Ducker, W., (1994). "Experimental Determination of Spring Constants in Atomic Force Microscopy" *Langmuir*, 10: 1003-1004.
3. Tortonese, M., Kirk, M., (1997). "Characterization of application-specific probes for SPMs. Micromachining and Imaging" *Micromachining and Imaging*, 53: 53-60.
4. Cumpson, P.J., Zhdan, P., Hedley, J. (2004) "Calibration of AFM cantilever stiffness: a microfabricated array of reflective springs" *Ultramicroscopy*, 100: 241-251.
5. Cumpson, P.J., Hedley, J., Zhdan, P. (2003) "Accurate force measurement in the atomic force microscope: a microfabricated array of reference springs for easy cantilever calibration" *Nanotechnology*, 14: 918-924.
6. Gibson, C.T., Watson, G.S., Myhra, S., (1996) "Determination of the spring constants of probes for force microscopy /spectroscopy" *Nanotechnology*, 7: 259-262.
7. Sader, J.E., White, L., (1993) "Theoretical analysis of the static deflection of plates for atomic force microscope applications" *Journal of Applied Physics*, 74: 1-9.
8. Cleveland, P., Manne, S., Bocek, D., Hansma, P.K. (1993) "A nondestructive method for determining the spring constant of cantilevers for scanning force microscopy". *Review of Scientific Instruments*, 64: 403-405.
9. Sader, J.E., Chon, J.W.M., Mulvaney, P., (1999) "Calibration of rectangular atomic force microscope cantilevers" *Review of Scientific Instruments*, 70: 3967-3969.
10. Hutter, J.L., Bechhoefer, J., (1993) "Calibration of atomic-force microscope tips" *Review of Scientific Instruments*, 64: 1868-1873.
11. Green, C. P., Lioe, H., Cleveland, J. P., Proksch, R., Mulvaney, P., Sader, J.E., (2004) "Normal and torsional spring constants of atomic force microscope cantilevers" *Review of Scientific Instruments*, 75: 1988-1996.
12. Sader, J. E., (1995) "Parallel beam approximation for V-shaped atomic force microscope cantilevers" *Review of Scientific Instruments*, 66: 4583-4587.
13. Burnham, N. A, Chen, X., Hodges, C. S., Matei, G. A., Thoreson, E. J., Roberts, C. J., Davies, M. C., S. J. B. Tandler (2003) "Comparison of calibration methods for atomic-force microscopy cantilevers" *Nanotechnology*, 14: 1-6.
14. Gates R. S. (2011) "Atomic Force Microscope Cantilever Flexural Stiffness Calibration: Toward a Standard Traceable Method" *National Institute of Standard Technology* 116: 703-727.
15. Neumeister, J. M., Ducker, W. A. (1994) "Lateral, normal, and longitudinal spring constants of atomic force microscopy cantilevers" *Review of Scientific Instruments*, 65: 2527-2531.
16. Sader, J. E., Green, C. P., (2004) "In-plane deformation of cantilever plates with applications to lateral force microscopy" *Review of Scientific Instruments*, 75: 878-883.
17. Cliffordand, C. A., Seah, M. P. (2005) "The determination of atomic force microscope cantilever spring constants via dimensional methods for nanomechanical analysis", *Nanotechnology*, 16: 1666-1680.
18. Sader, J. E., Sanelli, J. A., Adamson, B. D., Monty, J. P., Wei, X., Crawford, S. A., Friend, J. R. Marusic, I., Mulvaney, P., Bieske, E. J. (2012) "Spring constant calibration of atomic force microscope cantilevers of arbitrary shape" *Review of Scientific Instruments*, 2012. 83: 103705-103720.
19. Daeinabi, K., Korayem, M. H., Yarijani, S. A. (2011) "Spring constant analysis of the AFM rectangular, V-shaped and dagger cantilever probes" *Micro and Nano Letters*, 6: 1007-1011.
20. Daeinabi, K., Korayem, M. H., Yarijani, (2012) "Transducer Modeling of Rectangular, V-shaped, and Dagger Cantilever Probes Based on Atomic Force Microscopy" *Instrumentation Science and Technology*, 40: 338-354.

21. Li, R., Fan, K., Miao, J., Huang, Q., Tao, Sh., Gong, E. (2014) "An analogue contact probe using a compact 3D optical sensor for micro/nano coordinate measuring machines", *Measurement Science and Technology*, 24 : 094008.
22. Korayem, M. H., Taheri, M., Ghahnaviyeh, S. D. (2015) "Sobol method application in dimensional sensitivity analyses of different AFM cantilevers for biological particles" *Modern Physics Letter B*, 29:1550123.
23. Korayem, M. H., Ghaderi, R. (2014) "Dynamic modeling and vibration analysis of piezoelectric micro cantilever in AFM application", *International Journal of Mechanics and Materials in Design*, 10: 121-131